Impaired Wnt/β-catenin signaling disrupts adult renal homeostasis and leads to cystic kidney ciliopathy

Madeline A. Lancaster, Carrie M. Louie, Jennifer L. Silhavy, Louis Sintasath, Marvalyn DeCambre, Sanjay K. Nigam, Karl Willert, Joseph G. Gleeson

Supplementary Figure 1

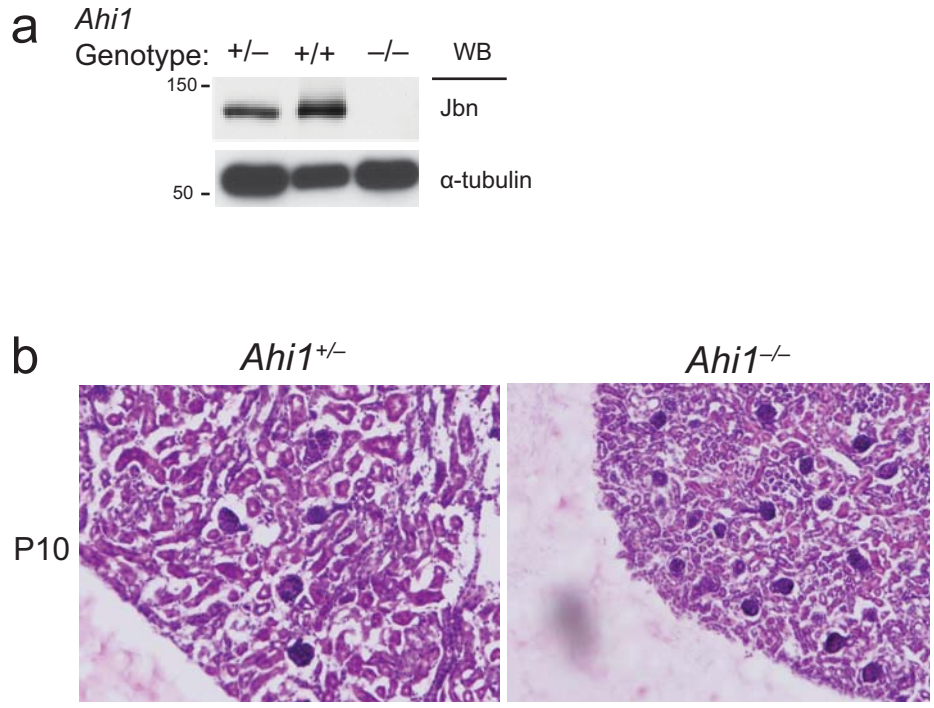

Supplementary Figure 1. *Ahi1*$^{-/-}$ analysis for the presence of Jbn protein. (**a**) Western blotting performed on brain lysates from littermates show complete lack of Jbn protein (exhibiting an approximate molecular weight of 125kDa) in *Ahi1*$^{-/-}$ samples and decreased levels in *Ahi1*$^{+/-}$ samples indicating complete loss of Jbn in the knockout and the specificity of the Jbn antibody. α-tubulin is shown as a loading control. (**b**) H&E staining of postnatal day 10 (P10) kidney sections from *Ahi1*$^{+/-}$ and *Ahi1*$^{-/-}$ littermates showing no clear differences in morphology.

Supplementary Figure 2

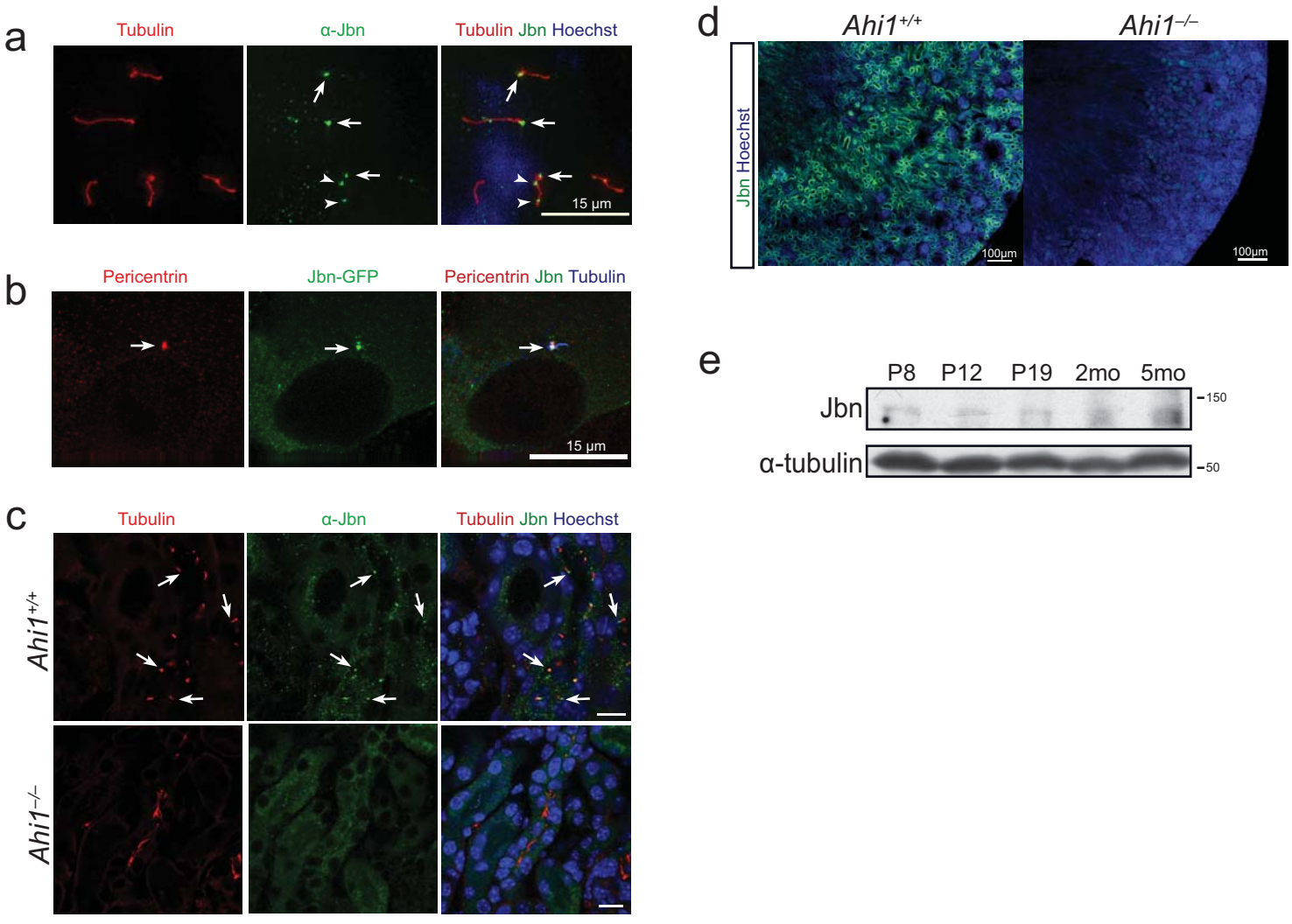

Supplementary Figure 2. Jouberin localizes primarily to the basal body *in vitro* and *in vivo*. (**a**) Staining for endogenous Jbn (green) in mIMCDs using the Jbn antibody reveals basal body (arrows) and ciliary punctate (arrowheads) staining. Acetylated tubulin (red) labels the cilium while Hoechst stains the nucleus. (**b**) GFP-tagged Jbn (green) co-localizes with pericentrin staining (red), a basal body marker. Acetylated tubulin staining is shown in blue. (**c**) Jbn antibody staining (green) in *Ahi1*$^{+/+}$ kidney tubules at 2 weeks of age reveals basal body localization (arrows) absent in the littermate *Ahi1*$^{-/-}$ kidney. (**d**) Low magnification image of Jbn antibody staining (green) in 2 week old kidney revealing high levels of expression in the cortex particularly adjacent to the medulla which is largely absent in *Ahi1*$^{-/-}$ littermate kidney. Hoechst stains the nuclei (blue). (**e**) Western blot analysis of Jbn expression in murine kidney which demonstrates increasing protein levels with age. α-tubulin is shown as a loading control.

Supplementary Figure 3

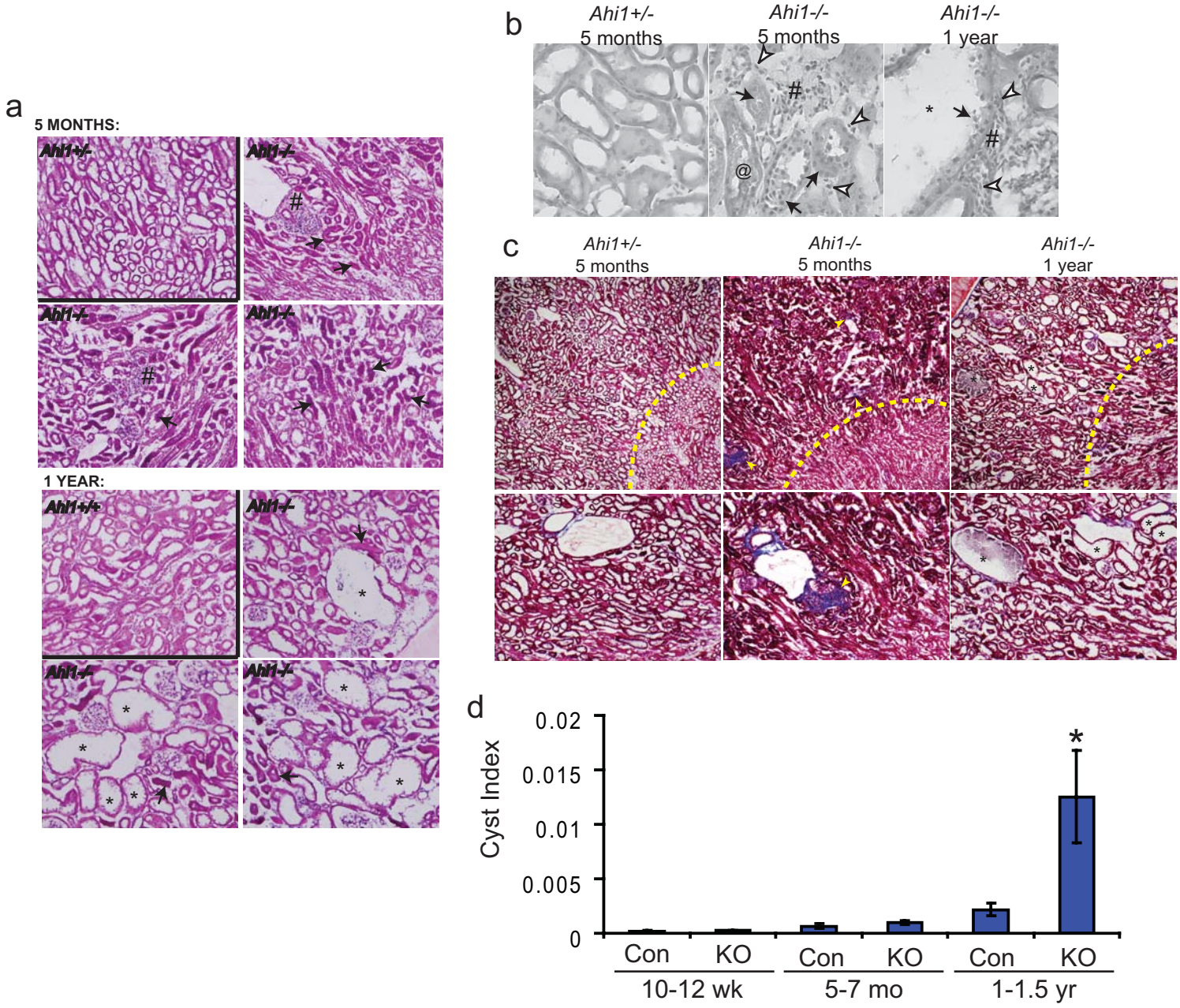

Supplementary Figure 3. *Ahi1*$^{-/-}$ kidneys display the characteristic features of NPHP. (**a**) H&E staining reveals early NPHP pathology in 5 month old *Ahi1*$^{-/-}$ kidney compared to *Ahi1*$^{+/-}$ littermate. Interstitial cell infiltrate (#) and fibrosis are present, as well as basement membrane abnormalities and tubular collapse (arrows). At one year, multiple microcysts and tubular dilatation become noticeable (*), and tubular basement membrane disintegration and atrophy are still present as well as tubular collapse (arrows) which are not evident in *Ahi1*$^{+/+}$ littermate control. (**b**) H&E staining at higher magnification which reveals properties of interstitial tissue. Again, tubule abnormalities are present (arrows) with collapsed tubules and thickened epithelial cell wall as well as deposits within the tubule lumen (@). Open arrowheads point to individual interstitial cells, which are part of a cluster of cell infiltrate (#). (**c**) Masson's trichrome further reveals tubular abnormalities including cystic dilation at 1 year (*) and aniline blue positive fibrosis (arrowheads). The large open structure visible in control and mutant 5 month sections is a blood vessel with nearby fibrosis. Dashed line represents the medullary boundary. (**d**) Average cyst index from three H&E stained sections of each kidney and both kidneys of at least 3 mice at each age. Control (Con, *Ahi1*$^{+/-}$ or *Ahi1*$^{+/+}$) littermates compared with *Ahi1* knockouts (KO). *P<0.05, Student's t-test.

Nature Medicine: doi:10.1038/nm.2010

Supplementary Figure 4

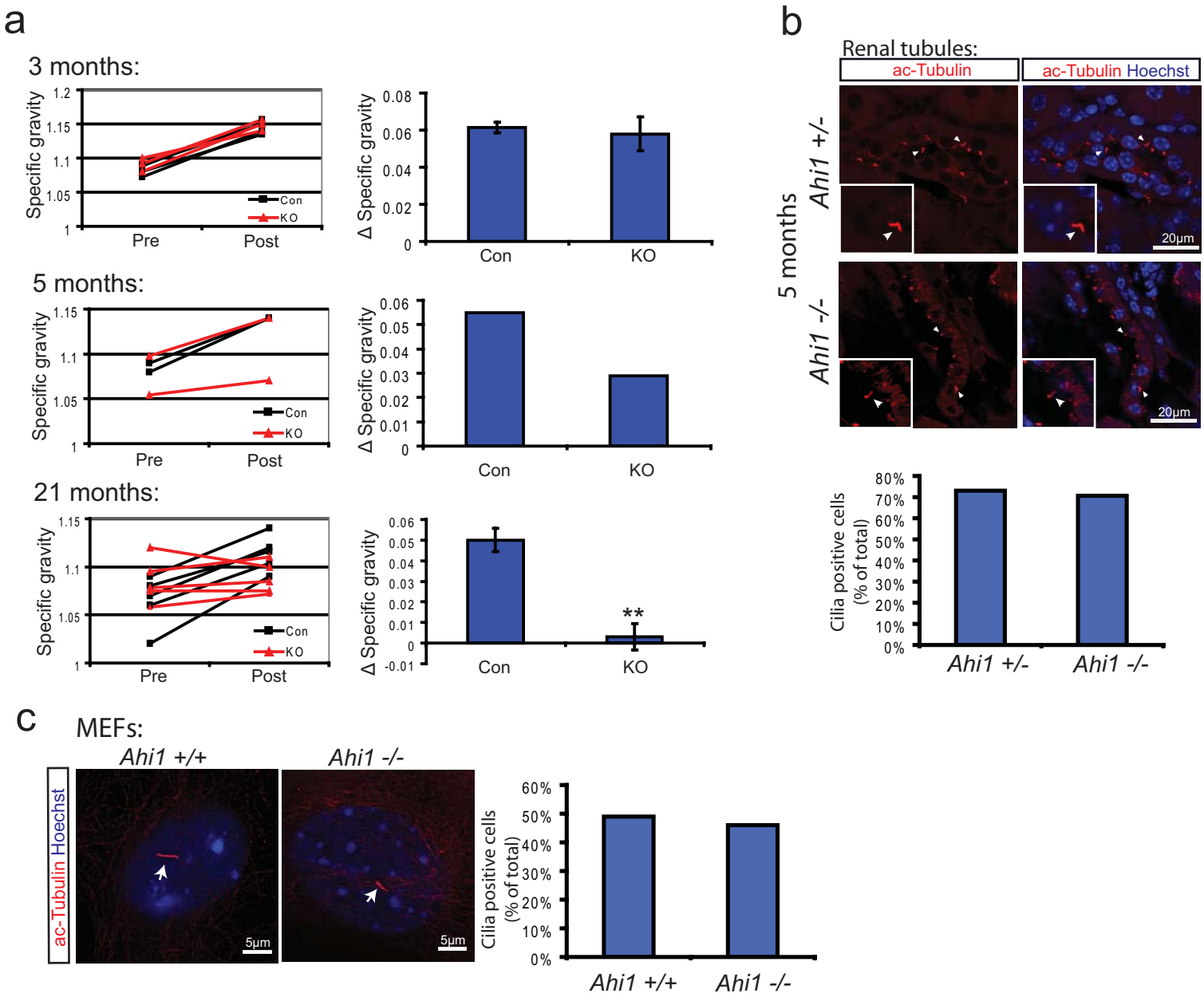

Supplementary Figure 4. *Ahi1*$^{-/-}$ display urine concentrating defects but normal percent ciliated MEFs and renal tubule cells. (**a**) Urine specific gravity measurements in *Ahi1*$^{-/-}$ and control littermates at 3 months, 5 months, and 2 years of age. Raw measurements before (Pre) and after (Post) dehydration are graphed at left while the average difference in specific gravity is graphed at right. ***P*<0.001, Student's *t*-test, n=5 mice at 21 months of age. (**b**) Staining for acetylated tubulin (red) reveals normal cilia number and morphology in *Ahi1*$^{-/-}$ kidneys compared with littermate control. Quantification of at least 100 cells from various tubule regions per sample reveals no significant difference in number of ciliated cells as determined by chi-squared test. (**c**) Mouse embryonic fibroblasts (MEFs) from *Ahi1*$^{+/+}$ and *Ahi1*$^{-/-}$ reveal normal cilia number and morphology. Quantitation of 100 MEF cells reveals no significant difference (chi-squared) in number of ciliated cells. Hoechst (blue) stains nuclei.

Supplementary Figure 5

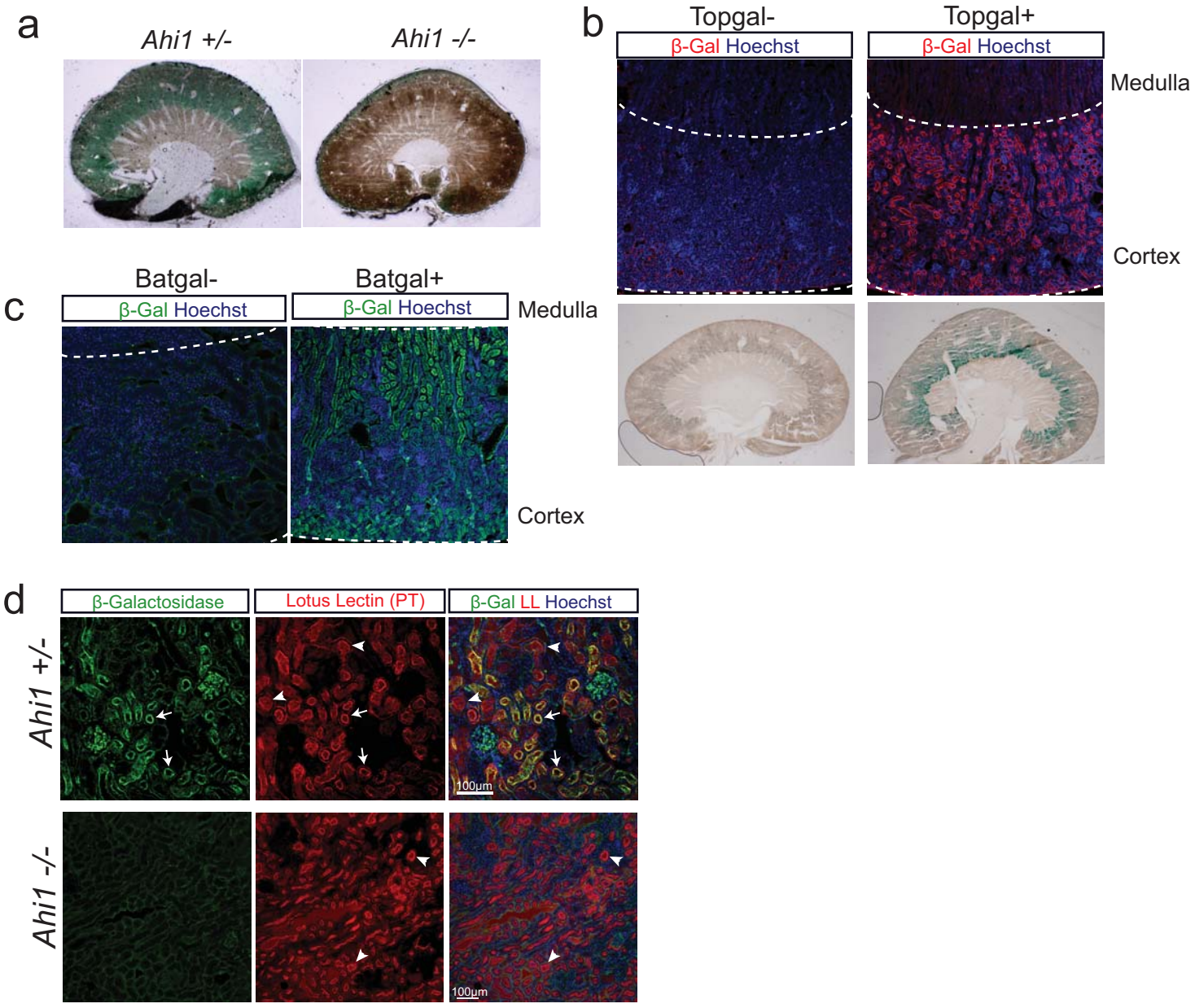

Supplementary Figure 5. *Ahi1*$^{-/-}$ kidneys display decreased Wnt activity. (**a**) X-Gal staining of *Ahi1*$^{+/-}$*; Tg+* and *Ahi1*$^{-/-}$*;Tg+* kidneys to saturation reveals a dramatic decrease in basal Wnt activity with loss of Jbn. (**b**) β-gal antibody staining (red) in wild-type Topgal negative kidney compared with Topgal positive kidney demonstrating the specificity of the Topgal reporter line. Dashed lines outline the cortex and Hoechst stains nuclei. Additionally, X-gal staining (at pH 7.7) was done in littermates revealing similar specificity of the reporter. (**c**) β-gal antibody staining (green) in an independent Wnt reporter line, Batgal, reveals similar cortical staining with highest activity proximal to the medulla. (**d**) β-gal (green) positive tubules colabel for lotus lectin (LL, red) which is a proximal tubule (PT) marker in *Ahi1*$^{+/-}$ kidney compared with *Ahi1*$^{-/-}$ littermate. Arrows point to the subset of proximal tubules which are co-positive for β-gal while arrowheads point to those which do not express β-gal. Despite the loss of β-gal expression in *Ahi1*$^{-/-}$, proximal tubules are still abundant. Hoechst (blue) marks nuclei.

Supplementary Figure 6

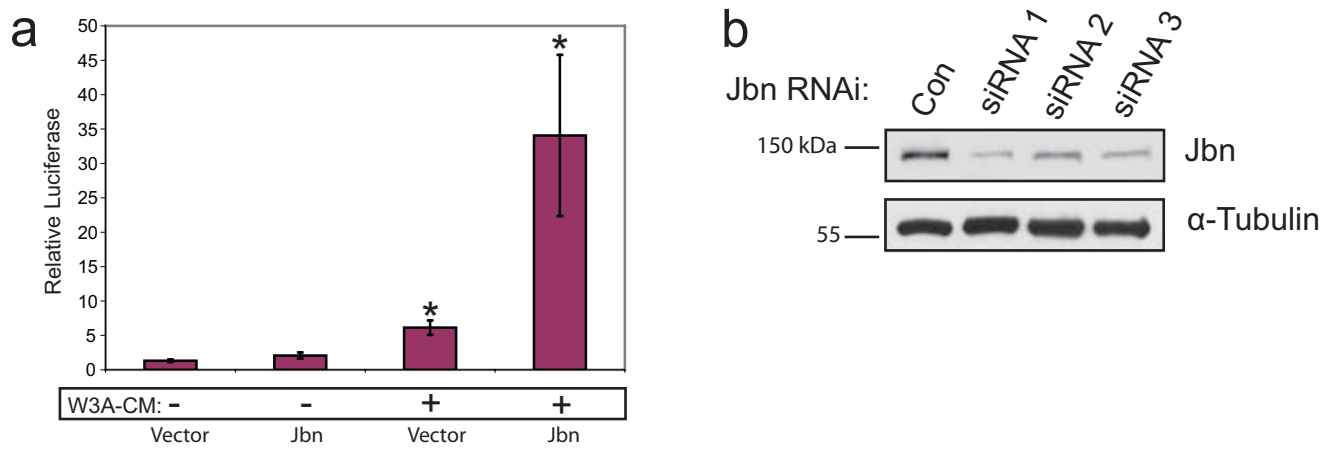

Supplementary Figure 6. Jbn overexpression potentiates the response to Wnt conditioned media. (**a**) 293T cells treated with Wnt3A conditioned media (W3A-CM) exhibit a 4.6-fold induction of luciferase response using the Topflash Wnt reporter. This response was potentiated by approximately 5.5-fold with Jbn overexpression. **P*<0.05, Student's *t*-test, n=12 from four experiments. Values were normalized for protein concentration and expressed as a ratio to the untreated vector condition. (**b**) N2A cells transfected with 3 different siRNA oligonucleotides exhibit decreased Jbn protein levels compared with negative control siRNA transfected. siRNA 1 and siRNA 3 show the most robust decreases.

Supplementary Figure 7

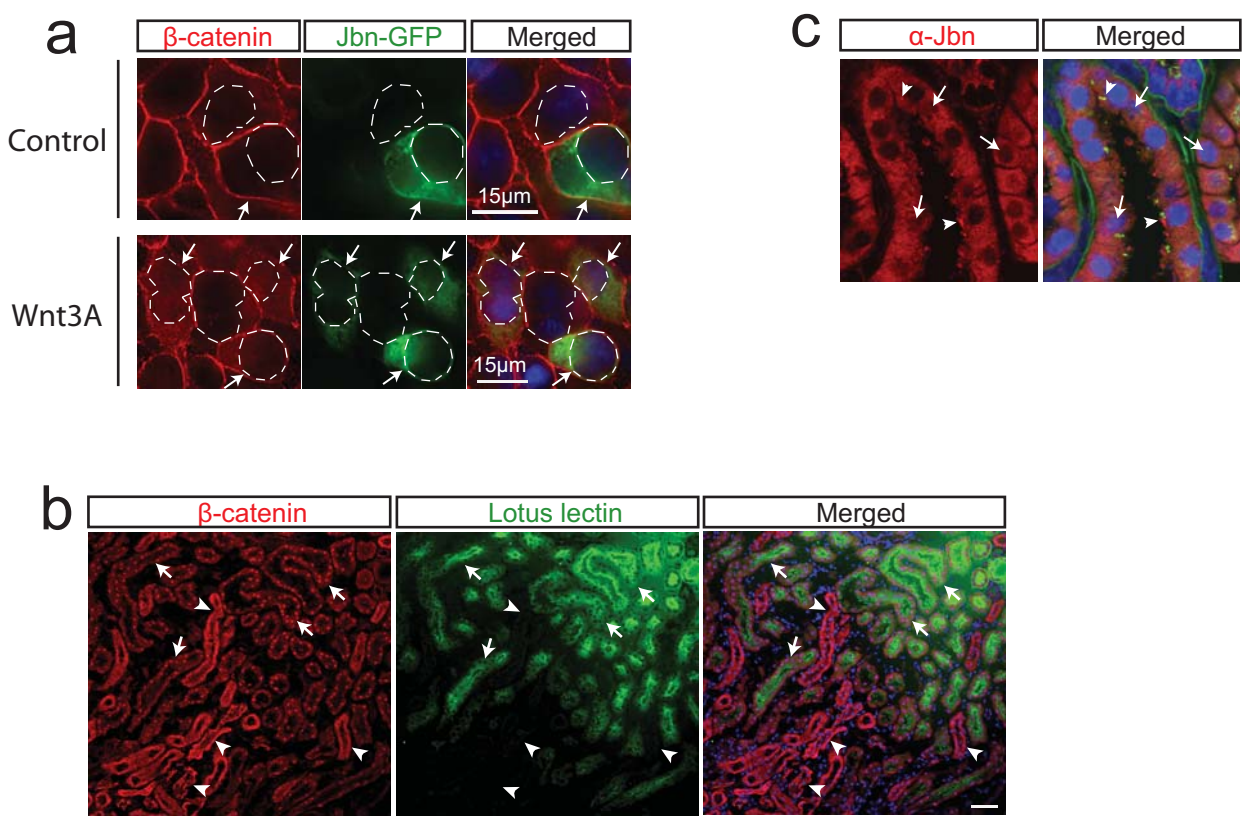

Supplementary Figure 7. Jouberin facilitates nuclear translocation of β-catenin (**a**) β-catenin localization in a single z-section through the plane of the nucleus in 293T cells reveals a subtle increase in nuclear levels of β-catenin (red) in cells overexpressing Jbn-GFP (green, arrows). Nuclei are labeled with Hoechst (blue) and are outlined by a dashed line. Jbn-GFP is not visible at the centrosome since it is out of the plane of focus. (**b**) β-catenin (red) and lotus lectin (green) costaining reveals nuclear localization of β-catenin in a subset of lotus lectin positive proximal tubules (arrows). Arrowheads point to tubules negative for lotus lectin which exhibit cytosolic and membrane β-catenin localization. (**c**) Immunostaining for Jbn (red) in kidney epithelium which demonstrates primarily cytosolic and basal body (arrowheads) localization at the base of acetyl-tubulin (green) positive cilia. Some nuclear punctate staining is visible as well (arrows). Hoechst (blue) labels nuclei.

Supplementary Figure 8

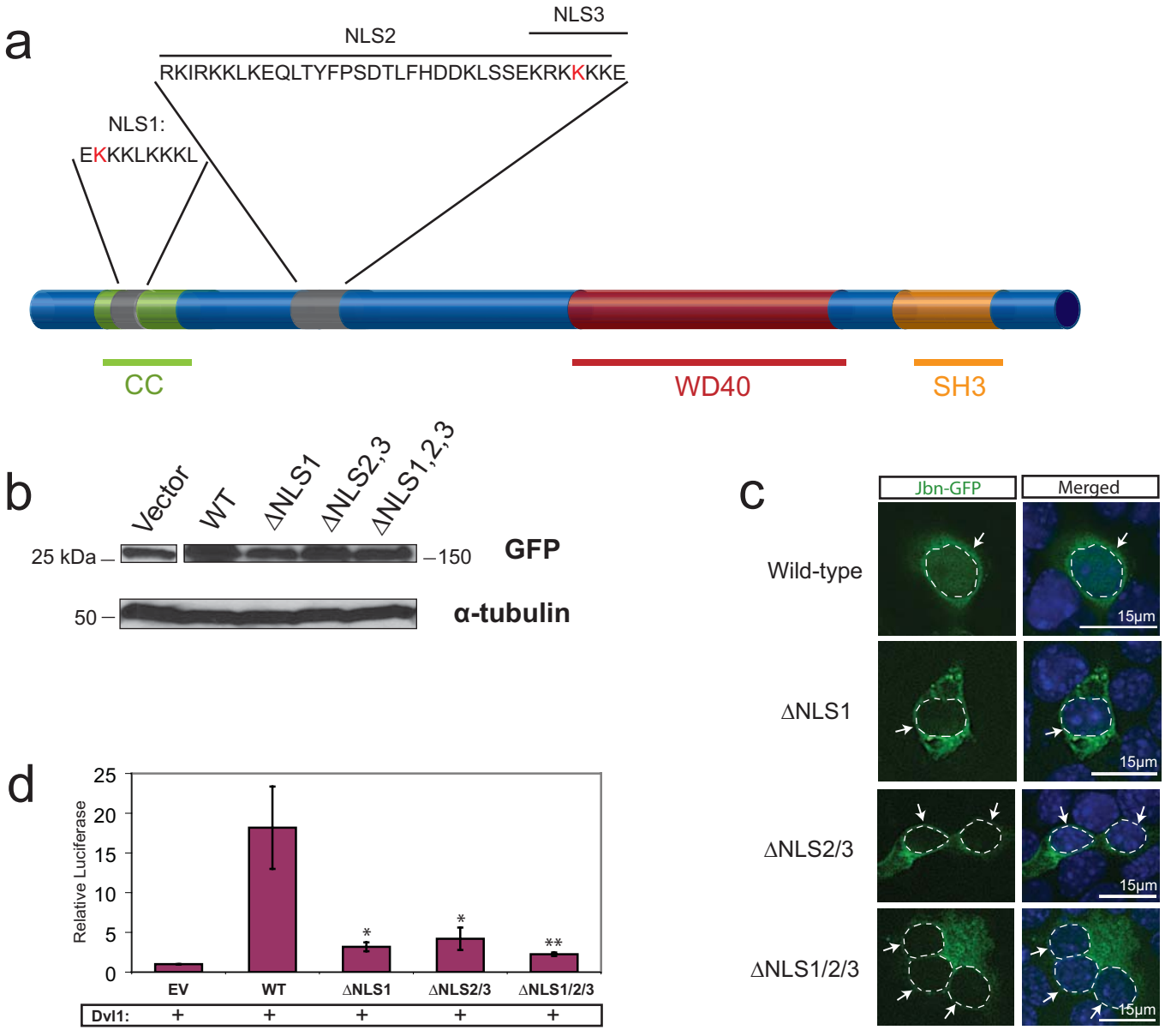

Supplementary Figure 8. NLS regions of Jbn are required for its Wnt function. (**a**) Schematic representation of Jbn with NLS sequences outlined. Mutated lysine residues are highlighted in red in NLS regions. CC = coiled-coil, WD40 = seven WD40 repeat region, and SH3 = SH3 binding domain. (**b**) 293T whole cell lysates transfected with NLS mutant constructs display comparable expression levels to wild-type as assayed by western blotting for GFP. α-tubulin is shown as a loading control. (**c**) Localization of NLS mutant EGFP constructs (green) in mIMCD cells. Nucleus (Hoechst, blue) is outlined by a dashed line. (**d**) Luciferase reporter activity in 293T cells transfected with Dvl-1 reveals a decrease in potentiation by NLS mutants compared to wild-type Jbn. **P*<0.05, ***P*<0.01, n=3 from three separate experiments, Student's *t*-test. Values are relative to empty vector control and were normalized for co-transfected β-Gal.

Supplementary Figure 9

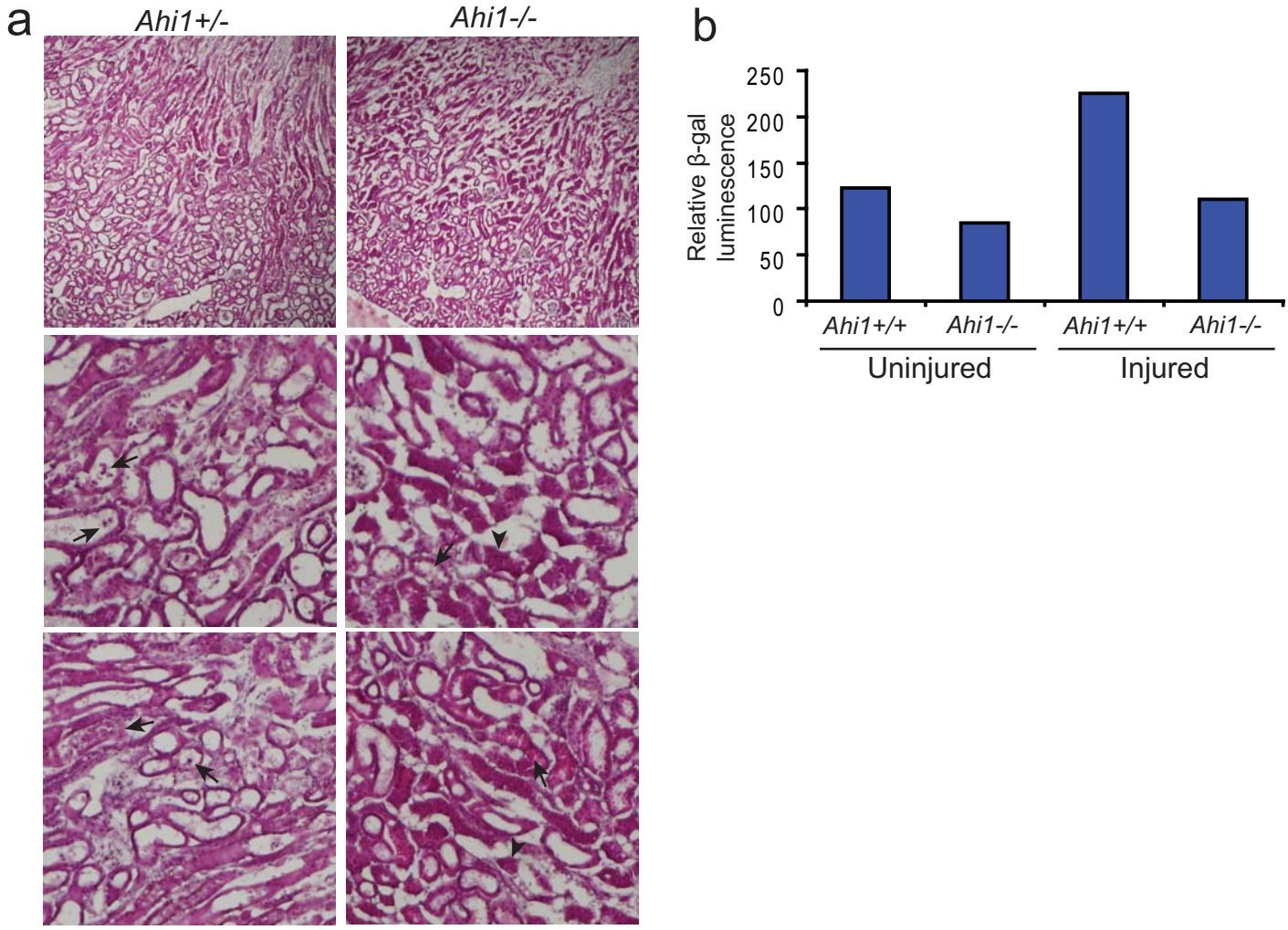

Supplementary Figure 9. Pathology immediately following injury in *Ahi1-/-* and *Ahi1+/-* kidney. (**a**) H&E staining of injured kidneys following unilateral IRI in $Ahi1^{-/-}$ and $Ahi1^{+/-}$ littermates aged 5 months. Signs of injury such as vacuolization and cell sloughing (arrows) are visible in both control and mutant injured kidneys. The $Ahi1^{-/-}$ kidney additionally exhibits the typical early manifestations of NPHP with some tubular abnormalities (arrowheads). (**b**) β-galactosidase luminescence relative to total protein concentration from whole kidney lysates of a pair of $Ahi1^{+/+}$ and $Ahi1^{-/-}$ littermates aged 3 months subjected to IRI revealing overall decreased Wnt activity even in the uninjured $Ahi1^{-/-}$ kidney at this early age prior to NPHP disease onset, and abrogated Wnt upregulation following injury compared with $Ahi1^{+/+}$ kidney lysate.

Supplementary Methods

Mouse line generation. We generated *Ahi1*$^{+/-}$ mice using homologous recombination (manuscript in preparation) and crossed them to TOPGAL^{+} mice[1] (JAX) to generate *Ahi1*$^{+/-}$; TOPGAL^{+} mice. F1 generation was then crossed to *Ahi1*$^{+/-}$ mice to generate *Ahi1*$^{-/-}$; TOPGAL^{+} and *Ahi1*$^{+/-}$; TOPGAL^{+} mice. We genotyped mice using primers for *Ahi1* and *LacZ* on tail DNA. We performed X-Gal staining using a previously published protocol[2] and maintaining a pH 7.7–8.0 to minimize endogenous activity[3,4]. Mouse work was carried out in compliance with Institutional Animal Care and Use Committee approved protocols.

Kidney injury. We performed kidney injury by either intraperitoneal injection of 20mg kg^{-1} body weight of cisplatin[5] or an equal volume/weight ratio of saline or by unilateral IRI similar to previously described[6]. Briefly, mice were anesthetized and the left kidney was exposed and subjected to vascular clamping for 30 min followed by removal of the clamp. The right kidney was left uninjured and animals were then sutured and allowed to recover.

Nuclear fractionation. We performed nuclear fractionation according to a previously published protocol[7], and nuclear coimmunoprecipitation was performed using rabbit antibody to GFP (Genetex) from nuclear extracts similarly prepared.

Transfection and luciferase assay. For transient transfections of 293T, mIMCD, Cos7, and N2A cells, we used Lipofectamine 2000 (Invitrogen) according to the manufacturer's protocol. For luciferase assays, we grew 293T cells and N2A cells in 12-well plates and transfected with 600 ng Topflash, 120 ng βGal, and 650 ng of Jbn-GFP expression plasmid or empty vector (GFP was mutated at Y66G to disrupt fluorescence using QuikChange mutagenesis). We co-transfected cells with 650 ng Dvl-1 expression plasmid, 650 ng β-CateninΔN, or treated with Wnt3a conditioned media (WCM) to stimulate the Wnt pathway. We obtained Wnt3A conditioned media from stably transfected L cells with Wnt3A expression vector and used as described[8]. Control media was from untransfected L cells. For experiments involving siRNA, we cotransfected

2.5pmol siRNA with half the above DNA amounts using Lipofectamine 2000 according to the manufacturer allowing for >80% transfection efficiency. 48 h following transfection, cells were serum starved for 16 h or treated with WCM diluted 3:1 in serum free media. We performed the luciferase assay according to a previously published protocol[9] and β-galactosidase activity was measured using the Tropix Galacto-light Plus kit (Applied Biosystems, T1007).

References

1. DasGupta, R. & Fuchs, E. Multiple roles for activated LEF/TCF transcription complexes during hair follicle development and differentiation. *Development* **126**, 4557-4568 (1999).
2. Yee, S.P. & Rigby, P.W. The regulation of myogenin gene expression during the embryonic development of the mouse. *Genes Dev* **7**, 1277-1289 (1993).
3. Duffield, J.S.*, et al.* Restoration of tubular epithelial cells during repair of the postischemic kidney occurs independently of bone marrow-derived stem cells. *J Clin Invest* **115**, 1743-1755 (2005).
4. Weiss, D.J., Liggitt, D. & Clark, J.G. Histochemical discrimination of endogenous mammalian beta-galactosidase activity from that resulting from lac-Z gene expression. *Histochem J* **31**, 231-236 (1999).
5. Megyesi, J., Safirstein, R.L. & Price, P.M. Induction of p21WAF1/CIP1/SDI1 in kidney tubule cells affects the course of cisplatin-induced acute renal failure. *J Clin Invest* **101**, 777-782 (1998).
6. Rabb, H.*, et al.* Renal ischemic-reperfusion injury in L-selectin-deficient mice. *Am J Physiol* **271**, F408-413 (1996).
7. Zambrano, N., Minopoli, G., de Candia, P. & Russo, T. The Fe65 adaptor protein interacts through its PID1 domain with the transcription factor CP2/LSF/LBP1. *J Biol Chem* **273**, 20128-20133 (1998).

8. Willert, K.*, et al.* Wnt proteins are lipid-modified and can act as stem cell growth factors. *Nature* **423**, 448-452 (2003).

9. Nelson, S.B., Lawson, M.A., Kelley, C.G. & Mellon, P.L. Neuron-specific expression of the rat gonadotropin-releasing hormone gene is conferred by interactions of a defined promoter element with the enhancer in GT1-7 cells. *Mol Endocrinol* **14**, 1509-1522 (2000).